

Original citation:

Aragó, Juan and Troisi, Alessandro. (2015) Excitonic couplings between molecular crystal pairs by a multistate approximation. *The Journal of Chemical Physics*, 142 (16). 164107.

Permanent WRAP url:

<http://wrap.warwick.ac.uk/74434>

Copyright and reuse:

The Warwick Research Archive Portal (WRAP) makes this work by researchers of the University of Warwick available open access under the following conditions. Copyright © and all moral rights to the version of the paper presented here belong to the individual author(s) and/or other copyright owners. To the extent reasonable and practicable the material made available in WRAP has been checked for eligibility before being made available.

Copies of full items can be used for personal research or study, educational, or not-for profit purposes without prior permission or charge. Provided that the authors, title and full bibliographic details are credited, a hyperlink and/or URL is given for the original metadata page and the content is not changed in any way.

Publisher's statement:

Copyright (2015) AIP Publishing. This article may be downloaded for personal use only. Any other use requires prior permission of the author and AIP Publishing.

The following article appeared in Aragó, Juan and Troisi, Alessandro. (2015) Excitonic couplings between molecular crystal pairs by a multistate approximation. *The Journal of Chemical Physics*, 142 (16). 164107 and may be found at <http://dx.doi.org/10.1063/1.4919241>

A note on versions:

The version presented here may differ from the published version or, version of record, if you wish to cite this item you are advised to consult the publisher's version. Please see the 'permanent WRAP url' above for details on accessing the published version and note that access may require a subscription.

For more information, please contact the WRAP Team at: publications@warwick.ac.uk



<http://wrap.warwick.ac.uk>

Excitonic couplings between molecular crystal pairs by a multistate approximation

Juan Aragó,* Alessandro Troisi

Department of Chemistry and Centre for Scientific Computing, University of Warwick,

Coventry CV4 7AL, UK

*E-mail: j.arago-march@warwick.ac.uk

In this paper, we present a diabaticization scheme to compute the excitonic couplings between an arbitrary number of states in molecular pairs. The method is based on an algebraic procedure to find the diabatic states with a desired property as close as possible to that of some reference states. In common with other diabaticization schemes this method captures the physics of the important short-range contributions (exchange, overlap and charge-transfer mediated terms) but it becomes particularly suitable in presence of more than two states of interest. The method is formulated to be usable with any level of electronic structure calculations and to diabaticize different types of states by selecting different molecular properties. These features make the diabaticization scheme presented here especially appropriate in the context of organic crystals, where several excitons localized on the same molecular pair may be found close in energy. In this paper the method is validated on the tetracene crystal dimer, a well characterized case where the charge transfer (CT) states are closer in energy to the Frenkel excitons (FE). The test system was studied as a function of an external electric field (to explore the effect of changing the relative energy of the CT excited state) and as a function of

different intermolecular distances (to probe the strength of the coupling between FE and CT states). Additionally, we illustrate how the approximation can be used to include the environment polarization effect.

I. INTRODUCTION

Exciton diffusion in molecular aggregates, films or crystals is mainly controlled by the excitonic coupling between the electronic excited states localized in the molecular units.¹ The excitonic coupling can be decomposed into different short-range (exchange, charge-transfer mediated and overlap) and long-range (Coulombic) contributions.^{2,3} One of the most widely used theoretical techniques to estimate the excitonic coupling between two molecules is the dipole-dipole scheme developed by Förster 65 years ago.⁴ This scheme is based on the electrostatic interaction between the transition dipole moments of the interacting molecules and can provide good estimates of the excitonic coupling as long as the spatial extension of the transition densities in the isolated molecules is smaller than the intermolecular distance. An improved scheme makes use of atomic transition charges instead of transition dipole moments.^{5,6} However, both schemes are only able to capture the long-range (Coulombic) contributions and should be carefully applied, for instance, in organic molecular crystals where the intermolecular distances are commonly found in the 3.5–4.5 Å range (van der Waals contacts). Recently, it has proven that the short-range contributions of the excitonic coupling turn out to be pivotal at van der Waals contacts⁷ and could in principle cause a large modulation of the excitonic coupling in molecular crystals as a consequence of thermal nuclear motion, analogous to what is found for the transfer integrals relevant for charge transport.⁸

Different diabaticization schemes have been successfully derived to estimate the total excitonic/electronic couplings (short- and long-range contributions).^{9–11} These schemes can be mainly divided into two groups: those based on the wavefunction and those based on molecular properties. Among the formers, the block diagonalization (BD),^{12,13}

developed by Pacher *et al.*, and the fourfold-way approach,¹⁴⁻¹⁶ developed by Nakamura and Truhlar, are the most popular and they have been widely applied in the field of photochemistry where conical intersections between different excited states need to be carefully characterized.^{17,18} In the BD approximation, a small set of adiabatic states is rotated by using the unitary transformation that minimizes the distance (in wavefunction space) between the desired diabatic states and a set of reference states which are nearly diabatic states (these reference states are assumed to be always available). The fourfold-way approximation is based on the construction of diabatic orbitals and the construction of many-electron diabatic states in terms of the previous diabatic orbitals. Although these wavefunction-based diabatization methods are rigorous, their implementation is not straightforward and depends on the nature of the wavefunction employed; for instance, the BD approach was only implemented in a complete active space self-consistent field (CASSCF) framework.^{19,20} Additionally, the extension for non wavefunction-based methodologies, such as the widely-used time-dependent density functional theory (TDDFT) approach or the methods based on the Bethe-Salpeter equation, is less straightforward. Therefore, these wavefunction-based diabatization schemes are limited to be used in small- or medium-size molecular systems where wavefunction methods can be applied.

In the context of electron or excitation energy transfer, the diabatization schemes based on molecular properties have become more popular.^{10,11} The main advantage of these diabatization schemes is that they can, in principle, be used independently of the level of theory. A particularly frequent choice among these diabatization schemes is the Generalized Mulliken-Hush (GMH) method,^{21,22} which is based on its predecessor method (the Mulliken-Hush model) and identifies the transformation that diagonalizes the adiabatic dipole moment matrix. When the transformation is applied to the adiabatic

(diagonal) Hamiltonian, the diabatic Hamiltonian is obtained and the excitonic couplings correspond to the off-diagonal elements of the diabatic Hamiltonian. Similar in spirit, Hsu *et al.* devised the fragment excitation difference (FED) scheme⁷ and Voityuk *et al.* a method that makes use of the transition dipole moments.²³ Very recently, a novel and general diabaticization scheme, based on dipole and quadrupole moments (called the DQ method), was developed by Hoyer *et al.* to compute electronic couplings between different electronic states.²⁴ This scheme is general and can be applied not only in the context of electron or energy transfer but also to states localized on the same molecule. Approximations based on the orbital localization approach of Boys,²⁵ and Edmiston and Ruedenberg²⁶ have been also developed by Subotnik and co-workers.^{27–29}

Alternative approaches to obtain excitonic/electronic couplings in the context of DFT have been also developed. The constrained density functional theory has been applied to compute excitonic couplings in relevant molecular systems.^{30–32} Pavanello and Neugebauer showed that the frozen density embedding subsystem formulation of density functional theory can also be a useful tool to estimate excitonic couplings between molecular moieties.^{33,34}

Although the methods presented above have been successfully applied for the study of excitonic (electronic) couplings in molecular systems, the majority of them are in general limited to the particular case where only two electronic states are involved and may therefore be difficult to apply in the presence of a third interacting electronic excited state close in energy to the two excited states of interest. Some methods able to calculate couplings beyond two electronic states^{27,35–37} in molecular aggregates are based on the definition of diabatic states (locally adiabatic states) that diagonalize the Hamiltonian for each subsystem (molecule). However, there are a large number of

examples where the state of interest is not localized on a single molecule. For instance, in molecular aggregates or crystals, charge-transfer (CT) excited states lie close in energy with respect to the low-lying singlet Frenkel (FE) excited states.³⁸ In the relevant cases of tetracene and pentacene crystals, the CT states are found to be only 0.35 and 0.29 eV above the lowest singlet FE state, respectively.³⁹ In fact, Yamagata *et al.* have shown that the lowest-energy singlet excitons in tetracene and pentacene crystals present a significant mixture of FE-type and CT-type excited states and that this FE-CT mixture may favour the exciton diffusion.⁴⁰ In this context, where CT states are close to the FE states, a diabaticization scheme capable of computing the total excitonic coupling (short- and long-range) between multiple excited states (e.g., between FE and CT states) would be very valuable. Additionally, it is important to note that the proper methodology to describe the nature of the lowest-energy excitons in these oligoacene crystals is still highly debated^{41–46} and, therefore, a diabaticization scheme insensitive to the level of theory would be also demanded.

Other interesting situations, where a multi-state diabaticization scheme would be required, may be those where the interacting molecular systems present degenerate or quasi-degenerate excited states. This is common for relevant molecular systems such as porphyrines,⁴⁷ coronenes,⁴⁸ and fullerene derivatives⁴⁹ as well as for polymeric systems where a large number of excited states close in energy can be found.^{50,51} Additionally, there are often dark states that need to be taken into account like the multi-excitonic state responsible for singlet fission in some materials.⁵² More generally, the representation of the excited state of a system as a linear combination of a small subset of interacting diabatic states is the key step for the construction of models for very large systems of interacting chromophores. The ability to generate such diabatic models with

a standardized procedure is therefore particularly useful for the most complex exciton physics problems that are currently under investigation.⁵³

In this paper, we present a general diabaticization scheme to compute the excitonic couplings between multiple excited states in molecular dimers. The diabaticization scheme is based on molecular properties, independent of the level of theory and, thus, particularly suitable in the context of organic molecular crystals. We present the results for the tetracene crystal dimer, a very well-studied case where an important mixture of FE and CT states in the lowest-energy singlet excitons is expected. The methodology will be used to explore the effect of the energy position of the CT state, the importance of the short-range interactions and the potential role of environmental polarization effects.

II. THEORETICAL MODELS AND COMPUTATIONAL DETAILS

A. Calculation of excitonic couplings in a general n -state approach

We consider a dimer system with n adiabatic singlet excited states of interest, $\{\psi_1^A, \psi_2^A, \dots, \psi_n^A\}$, with energies $\{E_1^A, E_2^A, \dots, E_n^A\}$. The diagonal (adiabatic) Hamiltonian matrix can be expressed as

$$\mathbf{H}^A = \begin{bmatrix} E_1^A & 0 & \dots & 0 \\ 0 & E_2^A & \dots & 0 \\ 0 & 0 & \ddots & 0 \\ 0 & 0 & \dots & E_n^A \end{bmatrix}. \quad (1)$$

The adiabatic excited states can be related to a set of diabatic excited states $\{\psi_1^D, \psi_2^D, \dots, \psi_n^D\}$ by means of an orthogonal transformation such as

$$\psi_i^D = \sum_j C_{ij} \psi_j^A. \quad (2)$$

The “best” diabatic wavefunctions have a very well defined *character* (e.g. Frenkel exciton localized on one molecule, charge transfer excitons) which is not modified by small changes in the system. There is not a unique way to define diabatic wavefunctions (sometimes called “quasi-diabatic”) and different prescriptions have been given in different contexts.^{9,10} The arbitrary nature of the diabatic basis is something that should be kept in mind and is ultimately related to a theorem demonstrated by Mead and Thrular on the impossibility of defining the ideal diabatic basis.⁵⁴

Once the orthogonal transformation matrix $\mathbf{C} = \{C_{ij}\}$ is determined, the adiabatic Hamiltonian (eq 1) can be related to the diabatic Hamiltonian as $\mathbf{H}^D = \mathbf{C}\mathbf{H}^A\mathbf{C}^T$, where \mathbf{C}^T is the transpose matrix of \mathbf{C} . The diagonal and off-diagonal elements of \mathbf{H}^D correspond to the diabatic energies (E_i^D) and the excitonic couplings (J_{ij}), respectively. Note that the diagonal and off-diagonal matrix elements of \mathbf{H}^D for the dimer system can be used to build an excitonic Hamiltonian for similar but larger molecular clusters.

Like in most diabatization schemes we wish to find the best unitary transformation \mathbf{C} that generates diabatic states as close as possible to reference states with a well-defined character (e.g. Frenkel excited states localized on a single molecule). For most excited states a property that allows monitoring the nature (localization, CT character) of the excited state is the set of atomic transition charges (ATC).⁵⁵ The adiabatic ATC matrix \mathbf{q}^A , where each column corresponds to the atomic transition charges of each excited state of interest ($\mathbf{q}_1^A, \mathbf{q}_2^A, \dots, \mathbf{q}_n^A$), is related to the diabatic ATC matrix \mathbf{q}^D by the unitary \mathbf{C}^T matrix,

$$\mathbf{q}^D = \mathbf{q}^A\mathbf{C}^T \quad (3)$$

We can assume that, using chemical intuition, it is possible to define the “ideal” diabatic electronic transition charge matrix ($\mathbf{q}^{D,\text{ref}}$), based on the atomic transition

charges of some reference systems (columns of the $\mathbf{q}^{\text{D,ref}}$ matrix, $\mathbf{q}_1^{\text{D,ref}}, \mathbf{q}_2^{\text{D,ref}}, \dots, \mathbf{q}_n^{\text{D,ref}}$). For example, a diabatic state localized on a molecule within a molecular dimer will have atomic transition charges very close to those computed for the isolated molecule. We discuss plausible choices for $\mathbf{q}^{\text{D,ref}}$ below and, in the remainder of this section, we assume that such reference $\mathbf{q}^{\text{D,ref}}$ can be constructed. We can define the best unitary transformation \mathbf{C} as the one making \mathbf{q}^{D} as close as possible to $\mathbf{q}^{\text{D,ref}}$. More formally, \mathbf{C} can be found as

$$\mathbf{C}^T = \arg \min_{\mathbf{R}} \left\| \mathbf{q}^{\text{A}} \mathbf{R} - \mathbf{q}^{\text{D,ref}} \right\| \quad (4)$$

where the symbol $\| \cdot \|$ denotes the square root of the sum of the square of all matrix elements (the Frobenius norm). The matrices \mathbf{q}^{A} and $\mathbf{q}^{\text{D,ref}}$ are rectangular matrices with a number of columns equal to the number of states of interest and a number of rows equal to the (much larger) number of atoms in the system. The problem in eq. 4 is a classical problem of linear algebra known as the orthogonal Procrustes problem,^{56,57} and admits a unique solution

$$\mathbf{C}^T = \mathbf{U} \mathbf{V}^T \quad (5)$$

where \mathbf{U} and \mathbf{V}^T are the matrixes resulting from the singular value decomposition (SVD)⁵⁸ of the matrix $\mathbf{M} = (\mathbf{q}^{\text{A}})^T \mathbf{q}^{\text{D,ref}} = \mathbf{U} \mathbf{\Sigma} \mathbf{V}^T$. The diabatic Hamiltonian, and therefore the excitonic couplings, is computed from \mathbf{C} as $\mathbf{H}^{\text{D}} = \mathbf{C} \mathbf{H}^{\text{A}} \mathbf{C}^T$. The main qualitative difference with respect to other methods used to generate diabatic states from molecular properties is that we have here an arbitrary number of properties (in this case a list of atomic transition charges), typically much larger than the number of states in the subspace of interest.

B. Computational details

Excitation energies and the atomic transition charges for the dimers and monomers of tetracene were calculated in the framework of the time-dependent density functional theory (TDDFT) by using the long-range corrected ω B97X-D^{59,60} density functional and the 6-31G* basis set. The ω B97X-D density functional has proven to provide an accurate description of valence and charge-transfer excitations in molecular dimers and avoids the typical underestimation of the charge-transfer excitations found in standard hybrid density functionals.⁶¹ In any case the methodology presented in this paper is independent from the choice of electronic structure calculation methods. All TDDFT calculations have been performed by using the Gaussian 09 program package.⁶²

III. RESULTS AND DISCUSSION

A. Coupling between FE and CT states in the presence of an external electric field

To validate our diabaticization scheme to compute excitonic couplings between more than two electronic excited states in molecular dimers, we have selected the tetracene dimer of the crystal unit cell (Figure 1a) as our first model system. The structure of the tetracene dimer has been directly extracted from the crystal structure and has not been optimized.⁶³ In the crystal cell dimer, we have computed the first adiabatic electronic transitions in the framework of TDDFT at the ω B97X-D/6-31G* level. The three lowest-energy adiabatic excited states are mainly described by combinations of one-electron promotions from the highest occupied molecular orbitals (HOMO and HOMO-1) to the lowest unoccupied molecular orbitals (LUMO and LUMO+1, see Figure 1b). A closer inspection of Figure 1 reveals that the two excited states S_1 and S_2 can be viewed as FE-type excited states (HOMO-1 \rightarrow LUMO and HOMO \rightarrow LUMO+1 configurations localized on each molecule) with a non-negligible mixture of a CT-type configuration (HOMO \rightarrow LUMO). The S_3 excited state corresponds to a CT

excited state (mainly described as a HOMO \rightarrow LUMO monoexcitation) with a mixture of the FE-type configurations. The nature of the three lowest-energy singlet excited states suggests that a significant coupling between the FE and CT excited states should take place in the crystal cell dimer of tetracene. These results are therefore in agreement with the findings reported by Yamagata et al. where it was shown that the nature of lowest-energy excitons in tetracene crystals has a significant mixture of FE-type and CT-type excited states.⁴⁰ It is also important to note that the two lowest-energy possible CT excited states in the dimer are not equivalent due to quadruple interactions⁶⁴ and, therefore, only the lowest-energy CT state is energetically closer to the lowest FE excited states and more mixed with them.

Although the discussion above has focused on the tetracene dimer of the crystal unit cell, other different dimers, for instance the slipped π -stacked dimer (Figure S1 in the supplemental material⁶⁵), can also be of great relevance to understand the exciton transport in the tetracene crystal. However, in the symmetric slipped π -stacked dimer of tetracene (similar to the symmetric slipped π -stacked dimer of pentacene⁶⁶), the lowest-energy excited states are FE-type states and CT excited states are not close in energy (Figure S1). Hence, for this symmetric dimer, only the coupling between the two lowest FE excited states needs to be computed and the multistate approximation presented here is easily simplified to a two-level approximation. Since our goal is to show the potential of the approximation to compute excitonic couplings in a complex scenario (when more than two excited states are close in energy), this symmetric dimer is only briefly discussed in the supplemental material.⁶⁵

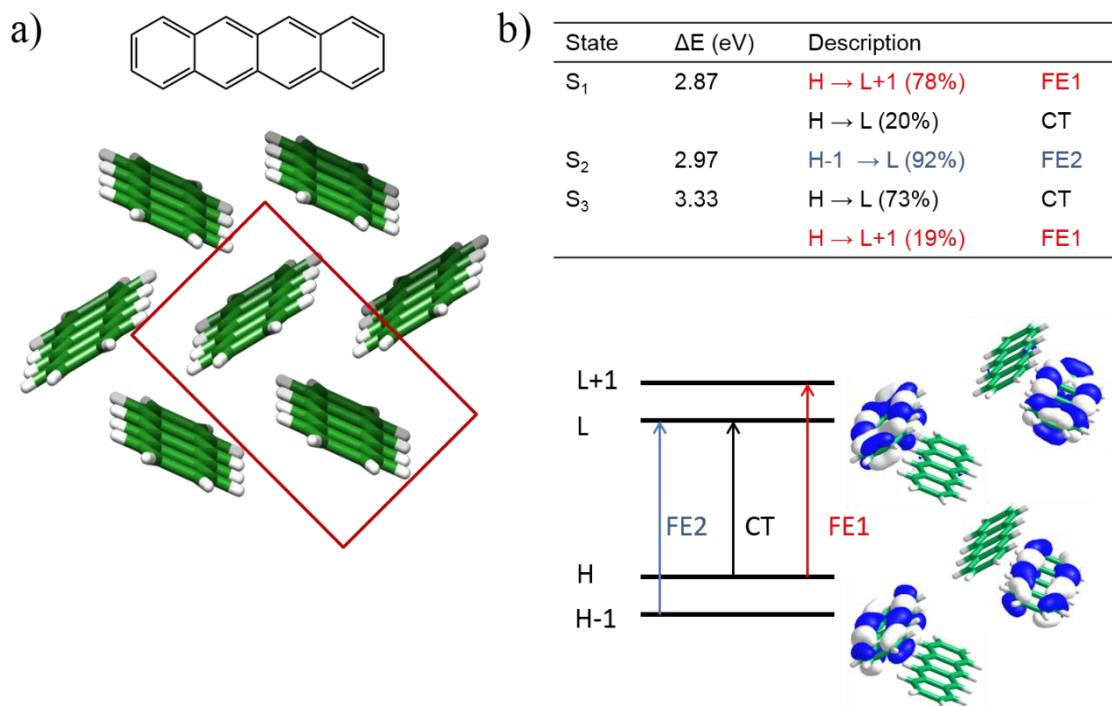


FIG. 1. (a) Chemical structure and herringbone crystal packing of tetracene. The tetracene dimer of the crystal unit cell is marked with a rectangle. (b) Energies and description of the three first excited states for the tetracene dimer at the crystal structure. H and L denotes HOMO and LUMO, respectively.

In the tetracene dimer, we are therefore interested in evaluating the excitonic coupling between two Frenkel excited states in the presence of a CT state. A very convenient test case is the tetracene dimer where an electric field is added in the direction parallel to the CT state dipole. The external electric field can be used to tune the energy of the CT state in relation with the FE states providing an ideal test for the role of CT states of different energies in molecular dimers. For this purpose, we carried out TDDFT calculations at the ω B97X-D/6-31G* level on the tetracene dimer and the respective monomers (at the geometry of the dimer) by using a variable electric field (F_y), where y is the direction connecting the centers of mass of the tetracene units in the dimer. The calculations on the dimer allow us to evaluate the adiabatic energies (E_1^A ,

E_2^A , and E_3^A) and atomic transition charges ($\mathbf{q}_1^A, \mathbf{q}_2^A$, and \mathbf{q}_3^A) for the first three singlet excited states (see the supplemental material⁶⁵ for the definition of ATCs). The “ideal” diabatic atomic transition charges for the two FE-type singlet excited states ($\mathbf{q}_{\text{FE1}}^{\text{D,ref}}$ and $\mathbf{q}_{\text{FE2}}^{\text{D,ref}}$) of the dimer were derived from the first singlet excited state on each monomer. In practice, to evaluate $\mathbf{q}_{\text{FE1}}^{\text{D,ref}}$, we computed ATCs for the first singlet excited state on isolated monomer 1 and set to zero the atomic transition charges on monomer 2. An analogous process is used to calculate $\mathbf{q}_{\text{FE2}}^{\text{D,ref}}$. ATCs for the “ideal” CT state ($\mathbf{q}_{\text{CT}}^{\text{D,ref}}$) were derived from the first singlet excited state of the dimer system in the limiting case where the CT state is much more stable than the FE states as a consequence of a strong external electric field ($F_y = -0.0050$ a.u.; 1 a.u. = 51.422 V Å⁻¹). In this case the CT state is not coupled with the FE states and, thus, can be considered as almost a pure CT state. Once the adiabatic energies, the adiabatic ATCs and the “ideal” diabatic ATCs are calculated, we have all the components needed for the construction of the diabatic states and their couplings.

Figure 2 compares the adiabatic and diabatic energies for the first three excited states as well as the excitonic couplings between them ($J_{\text{FE1-FE2}}$, $J_{\text{FE1-CT}}$, and $J_{\text{FE2-CT}}$) computed with the diabatization scheme as a function of F_y at the $\omega\text{B97X-D/6-31G}^*$ level. At electric fields in the 0.0010–0.0008 a.u. range, the nature of the first three adiabatic singlet excited states is similar to that previously discussed without electric field, that is, the first two excited states mainly correspond to FE-type states while the third excited state is a CT-type state (Figure 1b). In the region for F_y between -0.0008 to -0.0022 a.u., the description of S_1 , S_2 , and S_3 is more complicated owing to the significant mixture between the FE- and CT-type configurations. Below -0.0022 a.u., the nature of S_1 , S_2 , and S_3 becomes again simpler but now S_1 corresponds to the CT excited state whereas S_2 and S_3 are FE-type excited states, respectively. In the limit of $F_y = -0.0040$

a.u., the S_1 state is mainly described by only one HOMO \rightarrow LUMO monoexcitation, indicating that this state is almost decoupled with respect to S_2 and S_3 . The change of nature of the three adiabatic singlet excited states when F_y is switched on suggests that a crossing between the diabatic CT state with the diabatic FE states would need to take place. The analysis of the diabatic energies (Figure 2, middle panel) clearly reveals that the CT excited state is gradually stabilized with the electric field and becomes the first singlet excited state below -0.0018 a.u. In contrast, the diabatic energies of the FE excited states show almost no dependence on F_y . It should be noted that the diabaticization scheme predicts similar diabatic and adiabatic energies far from the crossing region.

The evolution of the excitonic coupling between the two FE states ($J_{FE1-FE2}$) and between the two FE states with the CT state (J_{FE1-CT} and J_{FE2-CT}) as a function of F_y (Figure 2, bottom) shows that all couplings present an almost linear behavior in the selected range of the electric field without discontinuities. The $J_{FE1-FE2}$ coupling remains almost constant with respect to the electric field, which is in agreement with the independent electric-field behavior of the diabatic energies for the two FE excited states (Figure 2, middle). J_{FE1-CT} and J_{FE2-CT} couplings tend to zero at negative values of F_y since, in this limit region, the CT state is energetically separated by more than 0.4 eV with respect to the FE excited states and is almost not coupled with the FE states. Note that the values of J_{FE1-CT} and J_{FE2-CT} in the limiting regions (F_y around -0.0040 or 0.0010 a.u.), where the CT state is well separated from the FE states, are less determining for the mixture between these excited states than close to the crossing region. This is, for example, confirmed for $F_y = 0.0010$ a.u. where relatively large J_{FE1-CT} and J_{FE2-CT} couplings are found but there is a small mixture between the FE and CT states.

In addition to the analysis of the evolution of the excitonic couplings with the electric field, it is also interesting to compare the excitonic couplings computed with the proposed diabaticization scheme for the tetracene dimer with some values reported in the bibliography. For instance, the largest excitonic coupling between the FE1 and CT states is -0.141 eV, which is in reasonable agreement with the excitonic coupling reported by Yamagata et al. (-0.076 eV).⁴⁰ Note that the difference between the two values can arise from the fact that the latter coupling was computed as the one-electron resonance integral between the monomers in the dimer of the crystal unit cell and at different DFT level (B3LYP/DZ). On the other hand, our value for $J_{\text{FE1-FE2}}$ (0.018 eV) is slightly larger than that reported for the same molecular dimer (0.011 eV).⁴⁰ This is something expected because the value in ref 38 included only the Coulomb term of the excitonic coupling whereas we have taken into account both the short- and long-range (Coulomb) effects with our diabaticization scheme. The comparison of the computed couplings with some values reported in the literature clearly illustrates that the predicted values computed here are found to be in a proper range. It is necessary to mention that we have developed a practical approach to deal with the problem of the coupling between multiple states with a reasonable accuracy but we are not interested in providing the most accurate coupling values for the tetracene dimer case, which may depend on the choice of the density functional and, therefore, on the position of the CT states. In fact, the prediction of excitation energies of CT states is a well-known problem in the standard TDDFT framework.⁶⁷ In this sense, the example presented above represents a meaningful test regardless of any potential inaccuracies of TDDFT as the energy of the CT state has been tuned by applying an electric field.

Although the excitonic couplings discussed so far have been computed by means of ATCs, it should be mentioned that similar excitonic couplings can be computed with

different molecular properties, for instance, transition dipole moments (see Table S1). Hence, the developed methodology can be accessible to experimentalists since physical observables as input parameters can be used. Additionally, it is worth mentioning that if dipole moments for the electronic states of interest were used, the methodology developed may be applied to compute electron-transfer couplings similar in spirit to the Generalized Mulliken-Hush approximation.²¹

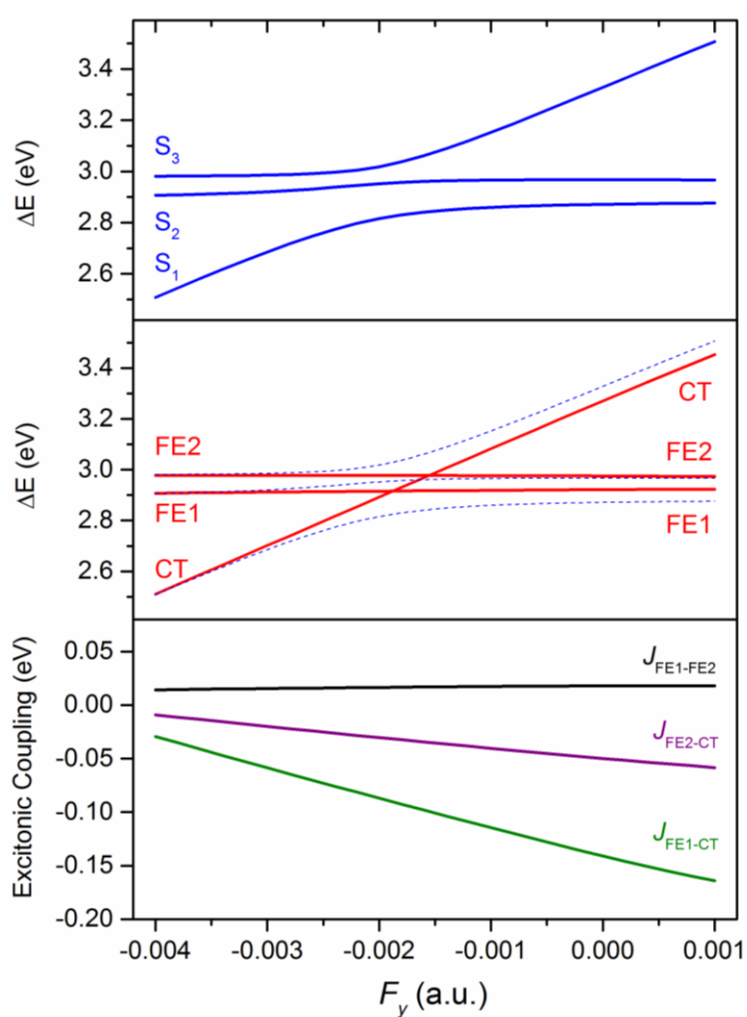


FIG. 2. Adiabatic (top) and diabatic (middle) energies of the first three singlet excited states as well as the excitonic couplings (bottom) computed for the crystal tetracene dimer as a function of the electric field (F_y) at the ω B97X-D/6-31G* level. Adiabatic energies have been also included in the middle panel for comparison purposes.

B. Inter-molecular distance dependence of the excitonic couplings

It has been shown that, when the intermolecular distance between the tetracene molecules of the crystal unit cell dimer decreases, a higher mixture between the FE and CT excited states occurs.⁶⁸ In this sense, we have applied the developed methodology to analyze the dependence of the excitonic couplings on the intermolecular distance in the crystal cell dimer of tetracene. Figure 3 shows the adiabatic and diabatic excitation energies computed for the three lowest energy singlet excited states as well as the $J_{\text{FE1-FE2}}$, $J_{\text{FE1-CT}}$, and $J_{\text{FE2-CT}}$ excitonic couplings as a function of the intermolecular distance. At distances larger than the crystal structure (3.7 Å), the first two excited states can be mainly described as FE-type states while the third one is a CT excited state (Figure 1b). At short intermolecular distances this simple description is no longer valid due to the significant mixture of FE and CT excited states. In the limit case analyzed (a very short intermolecular contact of 2.9 Å), the S_1 excited states is now a CT state and S_2 and S_3 correspond to the FE states. This trend is clear by analyzing the diabatic energies computed for the FE and CT excited states (Figure 3, middle) where the diabatic CT state is stabilized when decreasing the intermolecular distance. A crossing region between the two diabatic FE states and the diabatic CT state is found in the 3.2–3.4 Å range. Below 3.2 Å, the CT state becomes the lowest-energy singlet excited state. The FE-CT crossing has been also found for the case of the pentacene dimer in the context of singlet exciton fission.⁶⁹ The evolution of the $J_{\text{FE1-FE2}}$, $J_{\text{FE1-CT}}$, and $J_{\text{FE2-CT}}$ excitonic couplings as a function of the intermolecular distance (Figure 3, bottom) reveals that the absolute $J_{\text{FE1-FE2}}$, $J_{\text{FE1-CT}}$, and $J_{\text{FE2-CT}}$ couplings decrease as the intermolecular distance

increases, probably because of a decrease of the short-range contributions.⁷ For example, at large intermolecular distances (4.2 Å), the values computed for $J_{\text{FE1-FE2}}$, $J_{\text{FE1-CT}}$ and $J_{\text{FE2-CT}}$ (0.010, -0.096, and -0.028, respectively) are the smallest ones, which is in good agreement with the nature of the adiabatic states (almost no mixture between the three states) and with the large energy difference between the CT and the two FE states (more than 0.5 eV, Figure 3). It should also be noted that such an evaluation of the excitonic coupling from short to long distances demands the use of a methodology that treats short and long range coupling terms on the same footing, like the one proposed here.

An additional study to investigate the evolution of the excitonic coupling at very long intermolecular distances is given in the supplemental information⁶⁵ (Figure S2). The $J_{\text{FE1-FE2}}$ excitonic couplings exhibit the typical Coulombic decay ($\sim d^{-3}$) at very long distances, whereas the $J_{\text{FE-CT}}$ couplings decrease very quickly (as the orbital overlap) with the distance between the molecules. Figure S2 also shows the numerical stability of the method with a smooth variation of the diabatic matrix elements over the wide intermolecular distance range investigated. This robustness arises from the fact that the algebraic method guarantees a unique solution (i.e. the method is not based on a nonlinear optimization).

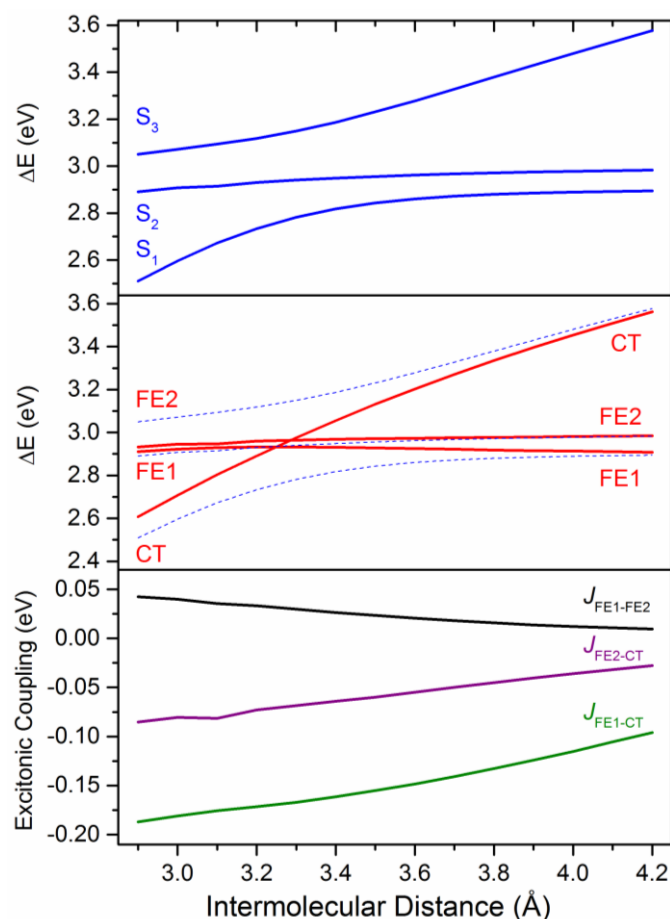


FIG. 3. Adiabatic (top) and diabatic (middle) energies of the first three singlet excited states as well as the excitonic couplings (bottom) computed for the crystal tetracene dimer as a function of the intermolecular distance at the ω B97X-D/6-31G* level. Adiabatic energies have been also included in the middle panel for comparison purposes.

Figure 4 compares the $J_{\text{FE1-FE2}}$ excitonic couplings computed within the three-state and the two-state approximation. At long intermolecular contacts ($> 4.0 \text{ \AA}$), the two approximations converge to the same value, although the two-state approach slightly underestimates the absolute value of the coupling. The agreement is expected since at these intermolecular distances the nature of the two first singlet excited states corresponds to unambiguous FE-type states. As the distance is reduced below 4.0 \AA , the

energy of the adiabatic states is influenced by the presence of a close CT state (Figure 3) and, therefore, a model that ignores the presence of this state will incorrectly capture the coupling between the FE states. Specifically the $J_{\text{FE1-FE2}}$ excitonic coupling in the two-state approximation appears to decrease until becoming negative and much larger in absolute value than the “correct” coupling evaluated with the three-state approximation. The approximation completely breaks down at very short intermolecular distances ($< 3.4 \text{ \AA}$) and the $J_{\text{FE1-FE2}}$ values become now positive because a change of the nature of the first excited state occurs; that is, the CT state becomes more stable than the FE states at short intermolecular distances and, thus, now the $J_{\text{FE1-FE2}}$ coupling should be computed between S_2 and S_3 instead of S_1 and S_2 as computed at long intermolecular distances. These findings clearly show that, in the situations where several excited states are close in energy and can interact together, a multi-state diabaticization scheme is highly recommended.

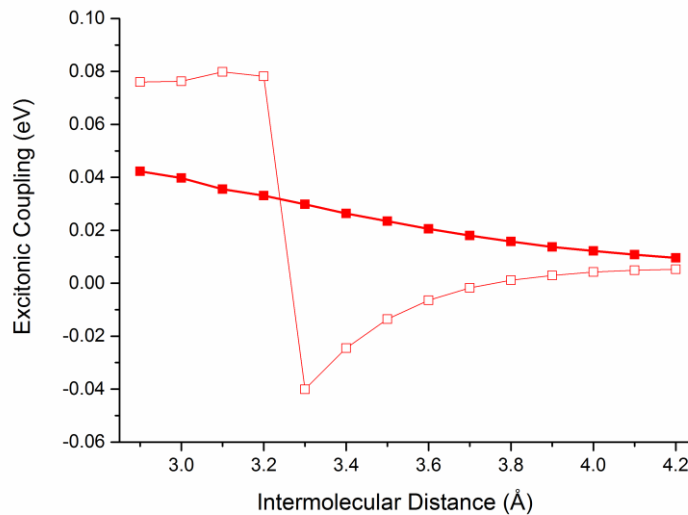


FIG. 4. Comparison of the $J_{\text{FE1-FE2}}$ excitonic couplings computed within the three- (solid squares) and two-state approach (open squares).

It should be noted that the reference states (i.e., the first singlet excited state of each monomer to calculate $\mathbf{q}_{\text{FE1}}^{\text{D,ref}}$ and $\mathbf{q}_{\text{FE2}}^{\text{D,ref}}$, and the first excited state of a dimer subject to an electric field to compute $\mathbf{q}_{\text{CT}}^{\text{D,ref}}$) are only computed once and, therefore, the sign of the excitonic coupling has been calculated consistently. This can be useful in several applications where the relative sign of the excitonic coupling does matter, including the divide-and-conquer schemes to evaluate the excitonic Hamiltonian of a large system from pairwise Hamiltonians.⁵³ **Figure S4** in the supplemental material⁶⁵ compares the $J_{\text{FE1-FE2}}$ couplings computed with three-state approximation and with the FED⁷ scheme. In the FED scheme, the sign of the excitonic coupling is not consistently computed and can fluctuate with the intermolecular distance. **Figure S4** also displays a breakdown for the FED scheme at short intermolecular distances, which is expected because this scheme computes the couplings only between two excited states and is unable to take into account the effect of a third state when it is close in energy to the two singlet excited states of interest.

C. Environment polarization effects

An interesting aspect to analyze is the possibility of capturing environment polarization effects through the diabaticization scheme proposed. To do so, the adiabatic energies and ATCs for the first three singlet excited states for the tetracene dimer of the crystal unit cell have been computed at the $\omega\text{B97X-D/6-31G}^*$ level in the presence of a polarizable continuum surrounding the molecules and described by the PCM model.⁷⁰

In combination with the TDDFT approximation, the PCM model is used in its standard linear response implementation (nonequilibrium) where it is assumed that the fast solvation degrees of freedom are equilibrated with the excited state density of the solute.

ATCs for the reference states ($\mathbf{q}_{\text{FE1}}^{\text{D,ref}}$, $\mathbf{q}_{\text{FE2}}^{\text{D,ref}}$ and $\mathbf{q}_{\text{CT}}^{\text{D,ref}}$) were computed as explained

above for the previous test cases. The effect of relative dielectric constant (ϵ_r) in the 1.0–7.0 range on the adiabatic and diabatic energies as well as the $J_{\text{FE1-FE2}}$, $J_{\text{FE1-CT}}$ and $J_{\text{FE2-CT}}$ couplings has been studied (Figure 5). Note that only the relative dielectric constant parameter has been varied and the rest of the specific parameters for the PCM model were the default ones for iodobenzene. The range for ϵ_r (1.0–7.0) has been selected to gain insight into the evolution of the excitonic couplings in the crystal environment since the relative dielectric constant is found to be around 4 in the tetracene crystal.⁴⁰ Figure 5 clearly reveals that the adiabatic energies (top panel) for S_1 and S_2 (mainly described as FE-type states) are hardly affected in the range of ϵ_r analyzed whereas a notable increase of the adiabatic energy (0.2 eV) as ϵ_r augments is found for S_3 (mainly a CT excited state). The latter finding seems to be unexpected but has been also found for the case of pentacene (Figure S5). This can be explained if the $J_{\text{FE1-CT}}$ coupling is analyzed in more detail (Figure 5, bottom), where $J_{\text{FE1-CT}}$ increases as a function of ϵ_r and, in principle, a larger mixture between the FE1 and CT states is expected. This is confirmed by the TDDFT calculations where a larger contribution of the diabatic FE1 configuration is present in S_3 (Figure S6). The increase of $J_{\text{FE1-CT}}$ can be also visualized in the computed diabatic energies (Figure 5, middle); while the energy for the diabatic FE2 state is predicted to be similar to that computed for S_2 , the energies for the diabatic FE1 and CT states are shifted respectively to higher and lower energies with respect to their homologous S_1 and S_3 adiabatic states. These results therefore suggest that, in the crystal environment, a larger mixture between FE and CT states than in vacuum is expected.

These findings highlight that the method presented to compute excitonic couplings can capture environment polarization effects without further modification, if such effects are sufficiently well described by a quantum chemical methodology that

incorporates polarization effects in the electronic structure calculation. There are several approximations that introduce solvent effects in the excitonic couplings in a more rigorous manner but the expressions used are more complicated and dependent of the density functional choice.⁷¹

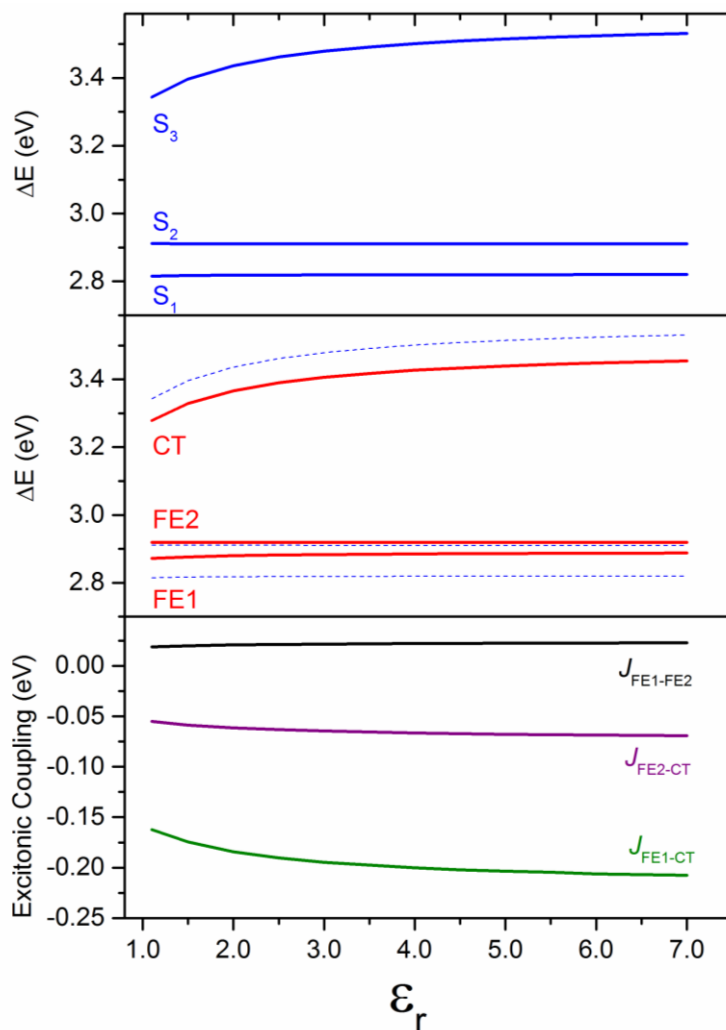


FIG. 5. Adiabatic (top) and diabatic (middle) energies of the first three singlet excited states as well as the excitonic couplings (bottom) computed for the crystal tetracene dimer as a function of dielectric constant (ϵ_r) at the ω B97X-D/6-31G* level. Adiabatic energies have been also included in the middle panel for comparison purposes.

IV. CONCLUSIONS

In this contribution, we have presented a novel diabaticization scheme to compute excitonic couplings between multiple excited states in molecular pairs. The scheme is based on an algebraic procedure (orthogonal Procrustes problem) to find the diabatic states with a desired molecular property as close as possible to that of some reference states. In addition to the possibility to deal with multiple excited states, the method is capable of capturing the physics of the important short-range (exchange, overlap and charge-transfer mediated terms) and long-range (Coulombic) contributions. These properties make the diabaticization scheme especially appropriate in the context of organic molecular crystals, where the short-range interactions are of special relevance and several excited states close in energy can be found. Furthermore, the diabaticization scheme is able to indirectly take into account solvent effects.

We have applied the developed diabaticization scheme to the particular case of the tetracene crystal dimer, which is a good example because the lowest Frenkel and charge-transfer singlet excited states are close in energy and they are mixed together. Our results reveal that the developed approximation can successfully predict the crossing region between the charge-transfer singlet excited state and the two lowest Frenkel singlet excited states in the two selected tests (by applying an external electric field and by decreasing the intermolecular distance). We have shown that the excitonic couplings computed within the three-state approximation present a continuous behavior and do not suffer from a breakdown as it is the case when only two states are considered. Additionally, we have shown that the coupling between one Frenkel state and a charge-transfer state is increased when augmenting the relative dielectric constant

of the solvent. This clearly indicates that solvent effects can be easily taken into account by the approximation presented.

ACKNOWLEDGEMENTS

This work was supported by a Marie Curie Intra European Fellowship within the 7th European Community Framework Programme (FP7-PEOPLE-2012-IEF-329513) and the European Research Council (Grant No. 615834). We are grateful to the Prof. E. Ortí (University of Valencia) for providing the computational facilities to perform the numerical calculations shown in this paper.

- ¹ V. May and O. Kühn, *Charge and Energy Transfer Dynamics in Molecular Systems* (Wiley-VCH Verlag GmbH & Co. KGaA, Weinheim, 2011).
- ² R.D. Harcourt, G.D. Scholes, and K.P. Ghiggino, *J. Chem. Phys.* **101**, 10521 (1994).
- ³ G.D. Scholes, R.D. Harcourt, and K.P. Ghiggino, *J. Chem. Phys.* **102**, 9574 (1995).
- ⁴ T. Förster, *Ann. Phys.* **437**, 55 (1948).
- ⁵ E. Hennebicq, G. Pourtois, G.D. Scholes, L.M. Herz, D.M. Russell, C. Silva, S. Setayesh, A.C. Grimsdale, K. Müllen, J.-L. Brédas, and D. Beljonne, *J. Am. Chem. Soc.* **127**, 4744 (2005).
- ⁶ S. Marguet, D. Markovitsi, P. Millié, H. Sigal, and S. Kumar, *J. Phys. Chem. B* **102**, 4697 (1998).
- ⁷ C.-P. Hsu, Z.-Q. You, and H.-C. Chen, *J. Phys. Chem. C* **112**, 1204 (2008).
- ⁸ A. Troisi and G. Orlandi, *J. Phys. Chem. A* **110**, 4065 (2006).
- ⁹ D.R. Yarkony, *Chem. Rev.* **112**, 481 (2012).
- ¹⁰ C.-P. Hsu, *Acc. Chem. Res.* **42**, 509 (2009).
- ¹¹ Z.-Q. You and C.-P. Hsu, *Int. J. Quantum Chem.* **114**, 102 (2014).
- ¹² T. Pacher, L.S. Cederbaum, and H. Köppel, *J. Chem. Phys.* **89**, 7367 (1988).
- ¹³ T. Pacher, L.S. Cederbaum, and H. Köppel, *Adv. Chem. Phys.* **84**, 293 (1993).
- ¹⁴ H. Nakamura and D.G. Truhlar, *J. Chem. Phys.* **115**, 10353 (2001).
- ¹⁵ H. Nakamura and D.G. Truhlar, *J. Chem. Phys.* **117**, 5576 (2002).

- ¹⁶ H. Nakamura and D.G. Truhlar, *J. Chem. Phys.* **118**, 6816 (2003).
- ¹⁷ H. Koppel, in *Conical Intersect. Electron. Struct. Dyn. Spectrosc.*, edited by W. Domcke, D.R. Yarkony, and H. Koppel (World Scientific, New Jersey, 2004), p. 175.
- ¹⁸ L.S. Cederbaum, in *Conical Intersect. Electron. Struct. Dyn. Spectrosc.*, edited by W. Domcke, D.R. Yarkony, and H. Koppel (World Scientific, New Jersey, 2004), p. 3.
- ¹⁹ W. Domcke, C. Woywod, and M. Stengle, *Chem. Phys. Lett.* **226**, 257 (1994).
- ²⁰ W. Domcke and C. Woywod, *Chem. Phys. Lett.* **216**, 362 (1993).
- ²¹ R.J. Cave and M.D. Newton, *Chem. Phys. Lett.* **249**, 15 (1996).
- ²² R.J. Cave and M.D. Newton, *J. Chem. Phys.* **106**, 9213 (1997).
- ²³ A.A. Voityuk, *J. Phys. Chem. C* **118**, 1478 (2014).
- ²⁴ C.E. Hoyer, X. Xu, D. Ma, L. Gagliardi, and D.G. Truhlar, *J. Chem. Phys.* **141**, 114104 (2014).
- ²⁵ S.F. Boys, in *Quantum Theory Atoms, Mol. Solid State*, edited by P.-O. Lowdin (Academic Press, New York, 1966), p. 253.
- ²⁶ C. Edmiston and K. Ruedenberg, *Rev. Mod. Phys.* **35**, 457 (1963).
- ²⁷ J.E. Subotnik, S. Yeganeh, R.J. Cave, and M.A. Ratner, *J. Chem. Phys.* **129**, 244101 (2008).
- ²⁸ J.E. Subotnik, R.J. Cave, R.P. Steele, and N. Shenvi, *J. Chem. Phys.* **130**, 234102 (2009).
- ²⁹ J.E. Subotnik, J. Vura-Weis, A.J. Sodt, and M.A. Ratner, *J. Phys. Chem. A* **114**, 8665 (2010).
- ³⁰ Q. Wu and T. Van Voorhis, *J. Chem. Phys.* **125**, 164105 (2006).
- ³¹ B. Kaduk, T. Kowalczyk, and T. Van Voorhis, *Chem. Rev.* **112**, 321 (2012).
- ³² S. Difley and T. Van Voorhis, *J. Chem. Theory Comput.* **7**, 594 (2011).
- ³³ J. Neugebauer, *J. Chem. Phys.* **126**, 134116 (2007).
- ³⁴ M. Pavanello and J. Neugebauer, *J. Chem. Phys.* **135**, 234103 (2011).
- ³⁵ R.J. Cave and M.D. Newton, *J. Phys. Chem. A* **118**, 7221 (2014).
- ³⁶ M. Rust, J. Lappe, and R.J. Cave, *J. Phys. Chem. A* **106**, 3930 (2002).
- ³⁷ C.-H. Yang and C.-P. Hsu, *J. Chem. Phys.* **139**, 154104 (2013).
- ³⁸ V.M. Agranovich, *Excitations in Organic Solids* (Oxford University Press, New York, 2009).
- ³⁹ L. Sebastian, G. Weiser, and H. Bässler, *Chem. Phys.* **61**, 125 (1981).

- ⁴⁰ H. Yamagata, J. Norton, E. Hontz, Y. Olivier, D. Beljonne, J.L. Brédas, R.J. Silbey, and F.C. Spano, *J. Chem. Phys.* **134**, 204703 (2011).
- ⁴¹ M.L. Tiago, J.E. Northrup, and S.G. Louie, *Phys. Rev. B* **67**, 115212 (2003).
- ⁴² K. Hummer and C. Ambrosch-Draxl, *Phys. Rev. B* **71**, 81202 (2005).
- ⁴³ P.M. Zimmerman, F. Bell, D. Casanova, and M. Head-Gordon, *J. Am. Chem. Soc.* **133**, 19944 (2011).
- ⁴⁴ P. Cudazzo, M. Gatti, and A. Rubio, *Phys. Rev. B* **86**, 195307 (2012).
- ⁴⁵ S. Sharifzadeh, P. Darancet, L. Kronik, and J.B. Neaton, *J. Phys. Chem. Lett.* **4**, 2197 (2013).
- ⁴⁶ B. Pac and P. Petelenz, *Chemphyschem* **15**, 2801 (2014).
- ⁴⁷ M. Gouterman, *The Porphyrines V3* (Academic Press, New York, 1978), pp. 1–156.
- ⁴⁸ G. Orlandi and F. Zerbetto, *Chem. Phys.* **123**, 175 (1988).
- ⁴⁹ D.M. Guldi and M. Prato, *Acc. Chem. Res.* **33**, 695 (2000).
- ⁵⁰ W. Barford, *Electronic and Optical Properties of Conjugated Polymers* (Oxford University Press, 2008).
- ⁵¹ H. Ma, T. Qin, and A. Troisi, *J. Chem. Theory Comput.* **10**, 1272 (2014).
- ⁵² M.B. Smith and J. Michl, *Chem. Rev.* **110**, 6891 (2010).
- ⁵³ J. Huh, S.K. Saikin, J.C. Brookes, S. Valleau, T. Fujita, and A. Aspuru-Guzik, *J. Am. Chem. Soc.* **136**, 2048 (2014).
- ⁵⁴ C.A. Mead and D.G. Truhlar, *J. Chem. Phys.* **77**, 6090 (1982).
- ⁵⁵ K.A. Kistler, F.C. Spano, and S. Matsika, *J. Phys. Chem. B* **117**, 2032 (2013).
- ⁵⁶ P.H. Schönemann, *Psychometrika* **31**, 1 (1966).
- ⁵⁷ J.C. Gower and G.B. Dijkstra, *Procrustes Problems* (Oxford University Press, New York, 2004).
- ⁵⁸ W.H. Press, S.A. Teukolsky, W.T. Vetterling, and B.P. Flannery, *Numerical Recipes 3rd Edition: The Art of Scientific Computing* (Cambridge University Press, Cambridge, U.K., 2007).
- ⁵⁹ J.-D. Chai and M. Head-Gordon, *Phys. Chem. Chem. Phys.* **10**, 6615 (2008).
- ⁶⁰ J.-D. Chai and M. Head-Gordon, *J. Chem. Phys.* **128**, 084106 (2008).
- ⁶¹ J. Aragó, J. Sancho-García, E. Ortí, and D. Beljonne, *J. Chem. Theory Comput.* **7**, 2068 (2011).
- ⁶² M.J. Frisch, G.W. Trucks, H.B. Schlegel, G.E. Scuseria, M.A. Robb, J.R. Cheeseman, G. Scalmani, V. Barone, B. Mennucci, G.A. Petersson, H. Nakatsuji, M. Caricato, X. Li, H.P.

Hratchian, A.F. Izmaylov, J. Bloino, G. Zheng, J.L. Sonnenberg, M. Hada, M. Ehara, K. Toyota, R. Fukuda, J. Hasegawa, M. Ishida, T. Nakajima, Y. Honda, O. Kitao, H. Nakai, T. Vreven, J.A. Montgomery, J.E. Peralta, F. Ogliaro, M. Bearpark, J.J. Heyd, E. Brothers, K.N. Kudin, V.N. Staroverov, R. Kobayashi, J. Normand, K. Raghavachari, A. Rendell, J.C. Burant, S.S. Iyengar, J. Tomasi, M. Cossi, N. Rega, J.M. Millam, M. Klene, J.E. Knox, J.B. Cross, V. Bakken, C. Adamo, J. Jaramillo, R. Gomperts, R.E. Stratmann, O. Yazyev, A.J. Austin, R. Cammi, C. Pomelli, J.W. Ochterski, R.L. Martin, K. Morokuma, V.G. Zakrzewski, G.A. Voth, P. Salvador, J.J. Dannenberg, S. Dapprich, A.D. Daniels, Farkas, J.B. Foresman, J. V Ortiz, J. Cioslowski, and D.J. Fox, Gaussian, Inc., Wallingford CT (2009).

⁶³ D. Holmes, S. Kumaraswamy, A.J. Matzger, and K.P.C. Vollhardt, *Chem. - A Eur. J.* **5**, 3399 (1999).

⁶⁴ D. Beljonne, J. Cornil, L. Muccioli, C. Zannoni, J.-L. Brédas, and F. Castet, *Chem. Mater.* **23**, 591 (2010).

⁶⁵ See supplemental material at for the expression of atomic transition charges, the lowest-energy excited states and its corresponding couplings of the slipped π -stacked tetracene dimer, comparison of the couplings computed with different properties, behavior of the couplings at very large intermolecular distances, and contribution of the main monoexcitations in the CT state as a function of the dielectric constant.

⁶⁶ P.B. Coto, S. Sharifzadeh, J.B. Neaton, and M. Thoss, *J. Chem. Theory Comput.* **11**, 147 (2014).

⁶⁷ A. Dreuw, J.L. Weisman, and M. Head-Gordon, *J. Chem. Phys.* **119**, 2943 (2003).

⁶⁸ D. Beljonne, H. Yamagata, J.L. Brédas, F.C. Spano, and Y. Olivier, *Phys. Rev. Lett.* **110**, 226402 (2013).

⁶⁹ T. Zeng, R. Hoffmann, and N. Ananth, *J. Am. Chem. Soc.* **136**, 5755 (2014).

⁷⁰ J. Tomasi, B. Mennucci, and R. Cammi, *Chem. Rev.* **105**, 2999 (2005).

⁷¹ C. Curutchet and B. Mennucci, *J. Am. Chem. Soc.* **127**, 16733 (2005).